Infotekmesin
Vol.14, No.02, Juli 2023
p-ISSN: 2087-1627, e-ISSN: 2685-9858
DOI: 10.35970/infotekmesin.v14i2.1919, pp. 318-326

The Influence of Fillet Step on Backward-Facing Step Flow Characteristics

James Julian[1*], Rizki Aldi Anggara[1], Fitri Wahyuni[1]
[1]Program Studi Teknik Mesin, Universitas Pembangunan Veteran Jakarta
[1]Jln. RS. Fatmawati Raya, Pd. Labu, Kec. Cilandak, Kota Depok, Jawa Barat 12450, Indonesia
E-mail: zames@upnvj.ac.id[1], rizky.aldianggara06@gmail.com[2], fitriwahyuni@upnvj.ac.id[3]

Info Naskah:
Naskah masuk: 28 Mei 2023
Direvisi: 3 Juli 2023
Diterima: 8 Juli 2023

Abstrak

Backward-facing step (BFS) merupakan model yang memberikan beberapa fitur yang aplikatif dibidang engineering. Fenomena yang kompleks pada aliran BFS memiliki dampak yang krusial untuk setiap bentuk penerapannya. Oleh karena itu, Penelitian ini menginvestigasi karakteristik aliran BFS secara komprehensif dengan variasi bentuk step yang berbeda. *Fillet backward facing step* (F-BFS) dipilih dan diuji pada interval Reynolds number 50 lebih kecil dari Re lebih kecil dari 400 melalui pendekatan CFD. Berdasarkan hasil komputasi, diperoleh bahwa *flow separation* merupakan bentuk fenomena yang fundamental pada aliran BFS. Akibat ekspansi mendadak, *flow separation* membentuk daerah resirkulasi yang terus meningkat hampir linear siring peningkatan bilangan Reynolds. Daerah resirkulasi mengandung vortex yang berputar secara tidak stabil sehingga dapat mempengaruhi efisiensi aliran BFS. Dengan menggunakan bentuk step yang berbeda, terbukti bahwa, F-BFS mampu meminimalisir daerah resirkulasi sehingga dapat meningkatkan efisiensi aliran BFS.

Keywords:
backward-facing step;
engineering
flow separation;
recirculation area;
vortex;

Abstract

Backward-facing step (BFS) is a model that provides several applicative features in engineering. The complex phenomena of BFS flow have a crucial impact on any application. Therefore, this study comprehensively investigates the flow characteristics of BFS with various step shapes. The backward-facing step (F-BFS) fillets were tested at intervals of Reynolds number 50 smaller than Re smaller than 400 using the CFD approach. Based on the computational results, it was found that flow separation is a fundamental phenomenon in BFS flow. Due to sudden expansion, Flow separation forms a recirculation area which continues to increase almost linearly with an increase in the Reynolds number. The recirculation area contains unstable rotating vortexes, which can impact the flow efficiency of BFS. Using a different step shape proves that F-BFS can minimize the recirculation area to increase the efficiency of the BFS flow.

***Penulis korespondensi:**
James Julian
E-mail: zames@upnvj.ac.id

1. Introduction

Backward-facing step (BFS) flow is one case that provides various forms of applicative function in engineering. Until now, the backward-facing step has had an essential role in both internal and external flows, such as aerospace engineering, heat transfer, flow control, and turbomachinery [1]–[4]. Fluid dynamics phenomena such as separation and reattaching of shear layers are a general form of fluid flow characteristics produced by BFS flow [5]. BFS uses simple geometry to form the steps in describing the flow phenomenon. Therefore, BFS is generally used as a general benchmark in understanding fluid dynamics phenomena to solve various problems in the field of engineering. Although the geometry used by BFS is quite simple, the resulting phenomena tend to be more complex. Thus, many studies have been conducted on various approaches to this phenomenon**.**

BFS has attracted the attention of various researchers because it has complex fluid flow properties for every application in the engineering field. There is research that investigates how to reduce the drag effect on hypersonic flow through a backward-facing step [6]. The research was conducted through numerical simulations with the Knudsen number 0.00009589. Based on the research, it was concluded that BFS is a geometry with a more significant drag effect than lift and can be minimized by increasing the step height in hypersonic vehicle designs as a form of implementing backward-facing step geometry. In addition, some studies carry out numerical investigations on turbulent flow passing through the BFS [7]. Traveling wave-like body force controls the fluid flow, which affects flow separation. Based on each case used in the control effect analysis, the average phase analysis shows a traveling wave effect on flow separation. Traveling wave generates upward flow, which can increase the rotation of the separation bubble. In addition, other studies have investigated the effects of transient flow through BFS with active flow control at high Reynolds numbers [8]. Active flow control is used to disrupt the shear layer and is proven to control flow separation and base pressure. The disturbed shear layer results in a significant decrease in reattachment length. In addition, high-frequency forcing can reduce the growth of shear layer instability and stabilize the latter half of the reattachment zone. This phenomenon allows for more upstream entrainment on a stepped base. This results in an increase in base pressure.

Based on several previous studies, the insight into knowing the fluid flow characteristics through the BFS is extensive. Separation of streams is the focus for researchers in maximizing the role of BFS for each form of its application. This study focuses on the flow characteristics of the BFS generated with different steps. By considering the importance of understanding related to BFS, the effect of step shape as one of the fundamental aspects is investigated with variations of the Reynolds number. The Backward Facing Step (F-BFS) fillet was chosen as the step shape, which has a radius so that the surface angle is smoother than the general form of the Backward Facing Step (BFS). In addition, fluid flow is described based on internal flow conditions. Therefore, this study provides insight into the characteristics of a wide range of fluid flows in in-channel flow applications.

2. Methodology

In this study, a literature study containing reference data sources in conducting research was carried out as a first step. The method in this study uses a numerical approach facilitated by Computational Fluid Dynamic (CFD) software. This method was chosen because it can describe the phenomenon accurately and economically. In the pre-processing stage, several parts consist of creating geometry, meshing, and determining boundary conditions. Furthermore, the realization stage is a computational process using CFD software. The result of this stage is in the form of data which will be continued to the post-processing stage. Data collection and grouping are carried out at this stage for the validation process. Numerical computational data results will be compared with experimental data from literature studies. If the data is invalid, the research process will return to the pre-processing stage. If the data is valid, the data will be analyzed as the next step to conclude the final result of the research. Overall, the flowchart in this study can be seen in Figure 1.

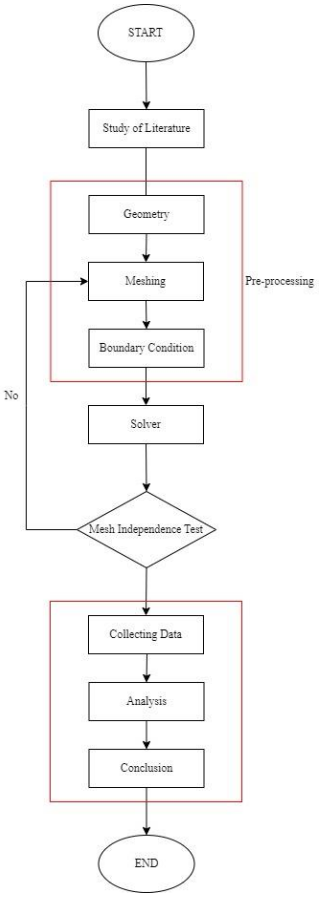

Figure 1. Research flow chart

2.1 Backward-Facing Step

The backward-facing step (BFS) is one of the fundamental representations of obstruction with a staircase geometry that gives specific characteristics to fluid flow. The formation of vortices and flow separation is a common

phenomenon that arises from the complex flow characteristics of BFS [9]. Reynolds number, step geometry, and fluid properties become parameters in determining fluid flow characteristics through the BFS. The fluid flow characteristics formed are based on the basic theory of the shear layer, which undergoes separation due to a staircase-shaped obstruction [10]. Generally, the BFS flow field can be divided into four regions: the separated shear layer, the recirculation region, the reattachment region, and the attached/recovery region [11]. The shear layer that undergoes separation will form a recirculation zone when it reaches a certain Reynolds number.

2.2 Geometries

This study describes the phenomenon of internal flow in two dimensions. Changes in the height of the channel are given to form the S rungs as a fluid domain. Changes in the height of the channel are set based on the expansion ratio H/h = 1.9423. The expansion ratio can be defined as the ratio between the downstream H channel height and the upstream h channel height. The expansion ratio in this study was chosen based on an experimental study conducted by Armaly [12].

In determining the expansion ratio mathematically, it can be seen in Equation (1). This study uses two variation models. The first model is the standard form of the backward-facing step (BFS) geometry. The second model is a backward-facing step geometry in a fillet (F-BFS) as an S step with a radius R as a comparison. The details of the two predefined geometries can be seen in Figure 2.

$$\frac{H}{h} = 1 + \frac{S}{h} \tag{1}$$

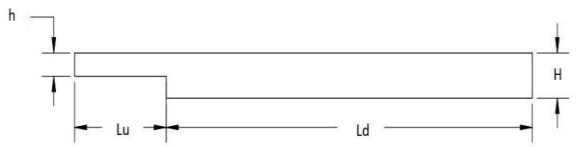

(a) Backward-facing step

(b) Fillet backward-facing step

Figure 2. Detail geometries

Table 1. parameter geometry

Parameter	Value (m)
h	0.5
H	0.97115
R	0.4
Lu	2.5
Ld	10

2.3 Governing Equation

This study uses Computational Fluid Dynamics (CFD) to solve numerically. Therefore, the Reynolds Averaged Navier-Stokes (RANS) equation is used as the Governing equation. The RANS equation consists of continuity and momentum equations of fluid flow which are functionally modified for CFD applications [13]–[15]. The RANS equation can be seen mathematically in Equations (2) and (3).

$$\frac{\partial \rho}{\partial t} + \frac{\partial}{\partial x_i}(\rho u_i) = 0 \tag{2}$$

$$\frac{\partial}{\partial t}(\rho u_i) + \frac{\partial}{\partial x_i}(\rho u_i u_j) = \frac{\partial p}{\partial x_i} + \frac{\partial}{\partial x_j}\left[\mu\left(\frac{\partial u_i}{\partial x_j} + \frac{\partial u_j}{\partial x_i} - \frac{2}{3}\delta_{ij}\frac{\partial u_i}{\partial x_i}\right)\right] + \frac{\partial}{\partial x_i}\left(-\rho\overline{u_i' u_j'}\right) \tag{3}$$

2.4 Mesh and Boundary Condition

This study uses a structured quadrilateral mesh type with mesh variations based on the number of elements in the meshing process. In addition, the Boundary conditions in the fluid domain are set to describe the phenomenon of internal flow through the BFS. This study uses a low Reynolds number variation, including; Re = 50, Re = 100, Re = 200, Re = 300, and Re = 400. The selection of the Reynolds number has been considered so that there is no effect of three-dimensional flow on the resulting phenomenon [12]. Boundary conditions on fluid flow are defined to represent fully developed laminar flow conditions on the channel as velocity-inlet, which forms a parabolic velocity profile, and zero pressure is defined as pressure-outlet. The inlet velocity is set based on Equations (4) and (5) using parameter D as the hydraulic diameter. In fulfilling the fully developed flow phenomenon, the ratio of maximum velocity (U_{max}) to average velocity (U_b) is set based on Equation (6). In addition, the boundary condition on the channel is defined as a no-slip wall divided into two parts, namely the upper and lower walls. On the lower wall, three areas represent the upstream wall, step wall, and downstream wall. Details of the mesh and boundary conditions can be seen in Figure 3.

$$\mathrm{Re} = \frac{\rho D U_b}{\mu} \tag{4}$$

$$D = 2h \tag{5}$$

$$U_{\max} = \left(\frac{3}{2}\right) U_b \tag{6}$$

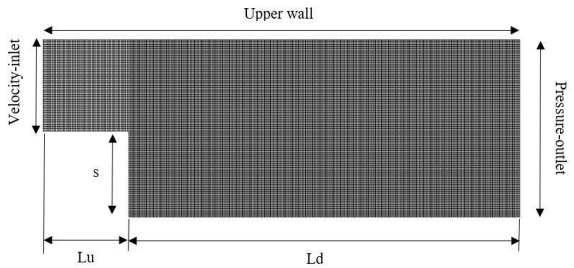

Figure 3. Detail mesh and boundary condition

2.5 Mesh Independence Test

Before the numerical simulation process, a mesh independence test is needed to determine the mesh with the smallest error value from the other mesh variations. Three mesh variations are defined based on the number of elements, namely, fine, medium, and coarse mesh. The fine mesh is defined as 100,000 elements. In addition, the medium mesh is defined as 80,000 elements. Meanwhile, for coarse mesh, the number of elements is 40,000.

In this study, the mesh independence test was carried out based on the application of research conducted by Roache [16]. The mesh independence test can be conducted by sampling the three mesh variations. The sample determined in the mesh independence test process is the fluid flow velocity at points x = 2.8 and y = 0. After sampling, the first step of the mesh independence test can be carried out by determining the ratio of mesh variations with Equation (7). After that, determining the order value of the mesh can be obtained through Equation (8) as the second step. In the third step, the error value in the predetermined mesh can be obtained by calculating the Grid Convergence Index (GCI), which is divided into two parts in Equations (9) and (10). GCI_{fine} is the error value between fine mesh and medium mesh. While GCI_{coarse} is the error value between the medium and coarse mesh. The variety of mesh used must be in the convergence area to prove that the GCI calculation on the mesh independence test is correct. After that, the process of calculating the error value for each mesh variation can be determined. Based on the calculation results of the mesh independence test, the mesh with the smallest error value is obtained by the fine mesh with an error value of 0.01020%. The results of the calculation of the mesh independence test can be seen in Table 2. Thus, the fine mesh is used in the numerical simulation process.

$$r = \frac{h_2}{h_1} \tag{7}$$

$$\bar{p} = \frac{\ln\left(\frac{f_3 - f_2}{f_2 - f_1}\right)}{\ln(r)} \tag{8}$$

$$GCI_{fine} = \frac{F_s \,|\in|}{\left(r^{\bar{p}} - 1\right)} \tag{9}$$

$$GCI_{coarse} = \frac{F_s \,|\in|\, r^{\bar{p}}}{\left(r^{\bar{p}} - 1\right)} \tag{10}$$

$$\in = \frac{f_{n+1} - f_n}{f_n} \tag{11}$$

$$\frac{GCI_{coarse}}{GCI_{fine} r^{\bar{p}}} \approx 1 \tag{12}$$

$$f\,r_{h=0} = f_1 + \frac{(f_1 - f_2)}{\left(r^{\bar{p}} - 1\right)} \tag{13}$$

Table 2. Grid independency study result

Mesh	Fine	Medium	Coarse
Velocity	0.00199549	0.00199600	0.00199779
$\bar{p}$		5.621803235	
r		1.25	
GCI_{fine}		0.013%	
GCI_{coarse}		0.0447%	
$f_{rh} = 0$		0.001995286	
$\frac{GCI_{coarse}}{GCI_{fine} r^{\bar{p}}}$		1	
Error	0.01020%	0.03576%	0.12537%

3. Result and Discussion

3.1 Validation

The data obtained from the numerical simulation results in this study was validated before proceeding to the analysis stage. Validation was carried out to ensure that the data obtained in this study stated the actual conditions. Therefore, a comparison of the two data between the experimental data and the simulation data was carried out. Experiment data obtained through research conducted by Almary is used as comparative data [12]. In the validation process, the change in the location of the reattachment point against the step height for each increase in the Reynolds number in the BFS flow with an expansion ratio H/h = 1.9423 is used as a sample, as seen in Figure 4. Based on the numerical simulation results, numerical data show satisfactory results similar to experimental data. The resulting trend curve shows a change in the location of the attachment point farther from the step as the Reynolds number increases. In addition, Table 3 shows the error value of the processing results, which shows an acceptable value. Thus, the simulation data obtained from this study are valid against actual conditions,

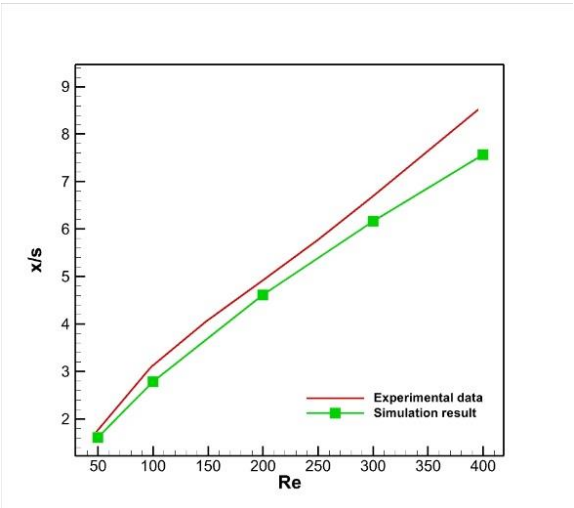

Figure 4. The location of the reattachment points behind the step normalized by the step height S

Table 3. Simulation error (%)

Re	Error (%)
50	7.108
100	9.853
200	5.674
300	7.525
400	11.203

3.2 Analysis

In this study, the effect of F-BFS on fluid flow characteristics was investigated within the range of Reynolds number 50<Re<400. The expansion ratio H/h = 1.9423 describes the rungs in the channel with a parabolic velocity profile. Boundary conditions that have been determined provide an overview of fully developed internal flows. In Figure 5, the contour Streamwise velocity is given to visualize the characteristics of the fluid flow passing through the BFS. It can be seen that velocity has the maximum value on the upstream side. The decrease in velocity near the wall in the channel is caused by a viscosity effect characterized by two fused boundary layers. The boundary layer that is formed is then separated from the wall surface of the channel when passing through the step to form a flow separation. Flow separation occurs because the fluid flow cannot follow the geometry due to sudden expansion changes. In Figure 5, it can be seen that F-BFS can minimize the flow separation that occurs. F-BFS has a smoother angle when compared to BFS so that the fluid flow still has the momentum to flow following the channel's geometric surface shape.

The boundary layer that is separated due to changes in the expansion will cause the fluid flow outside the boundary layer to accelerate. This condition can be seen in Figure 6, which shows the contour transverse velocity. Transverse velocity is a fluid velocity component with a direction perpendicular to the surface of the channel. After passing through the flow separation area, the fluid that returns to touch the surface will interact to re-form the boundary layer. Therefore, it can be observed that the fluid experiences velocity to move away from the two wall surfaces towards the center line in the channel until it finally disappears after the fluid flow returns to being fully developed.

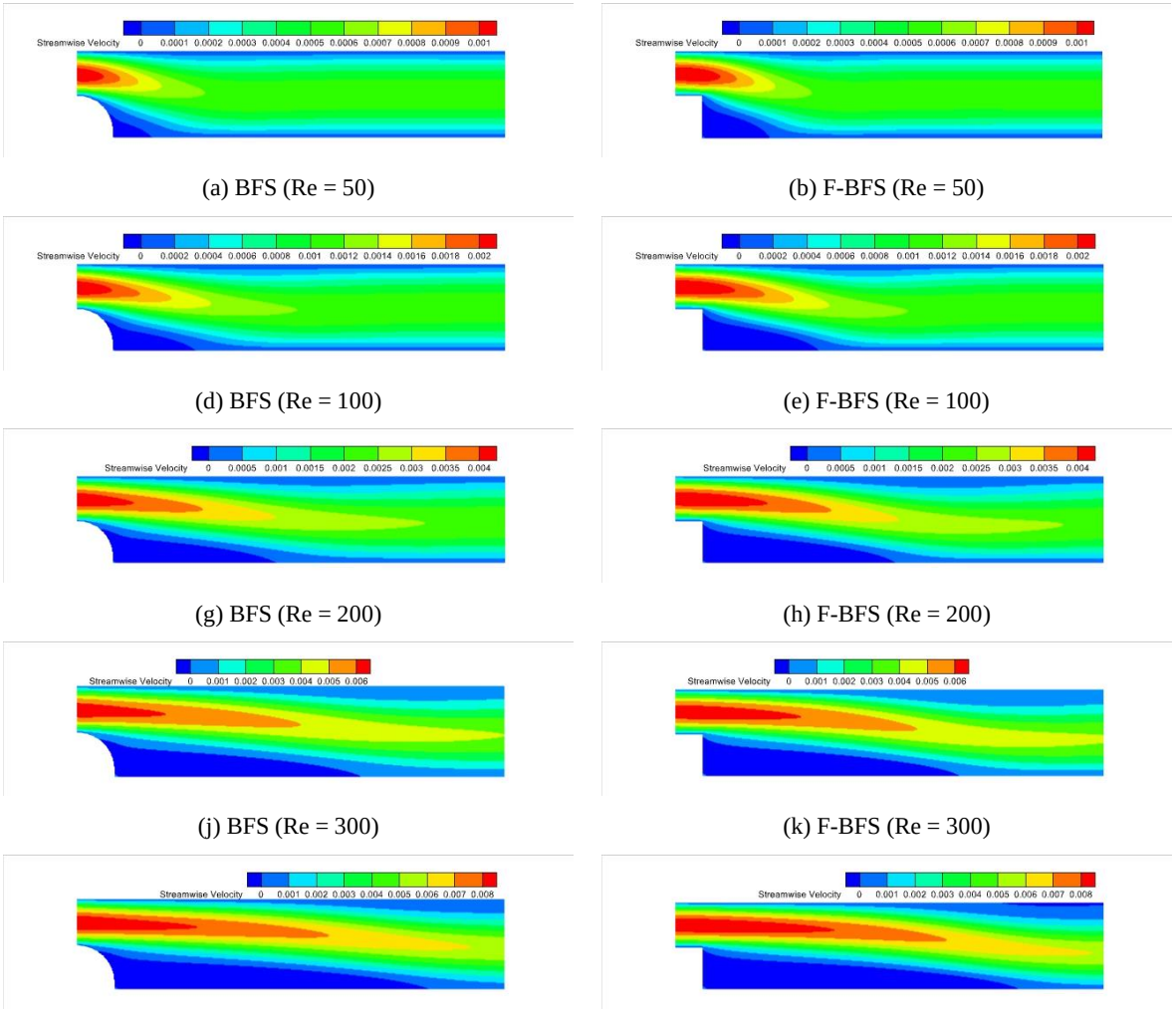

(a) BFS (Re = 50) (b) F-BFS (Re = 50)

(d) BFS (Re = 100) (e) F-BFS (Re = 100)

(g) BFS (Re = 200) (h) F-BFS (Re = 200)

(j) BFS (Re = 300) (k) F-BFS (Re = 300)

(l) BFS (Re = 400) (m) F-BFS (Re = 400)

Figure 5. Streamwise velocity contour of backward facing step flow

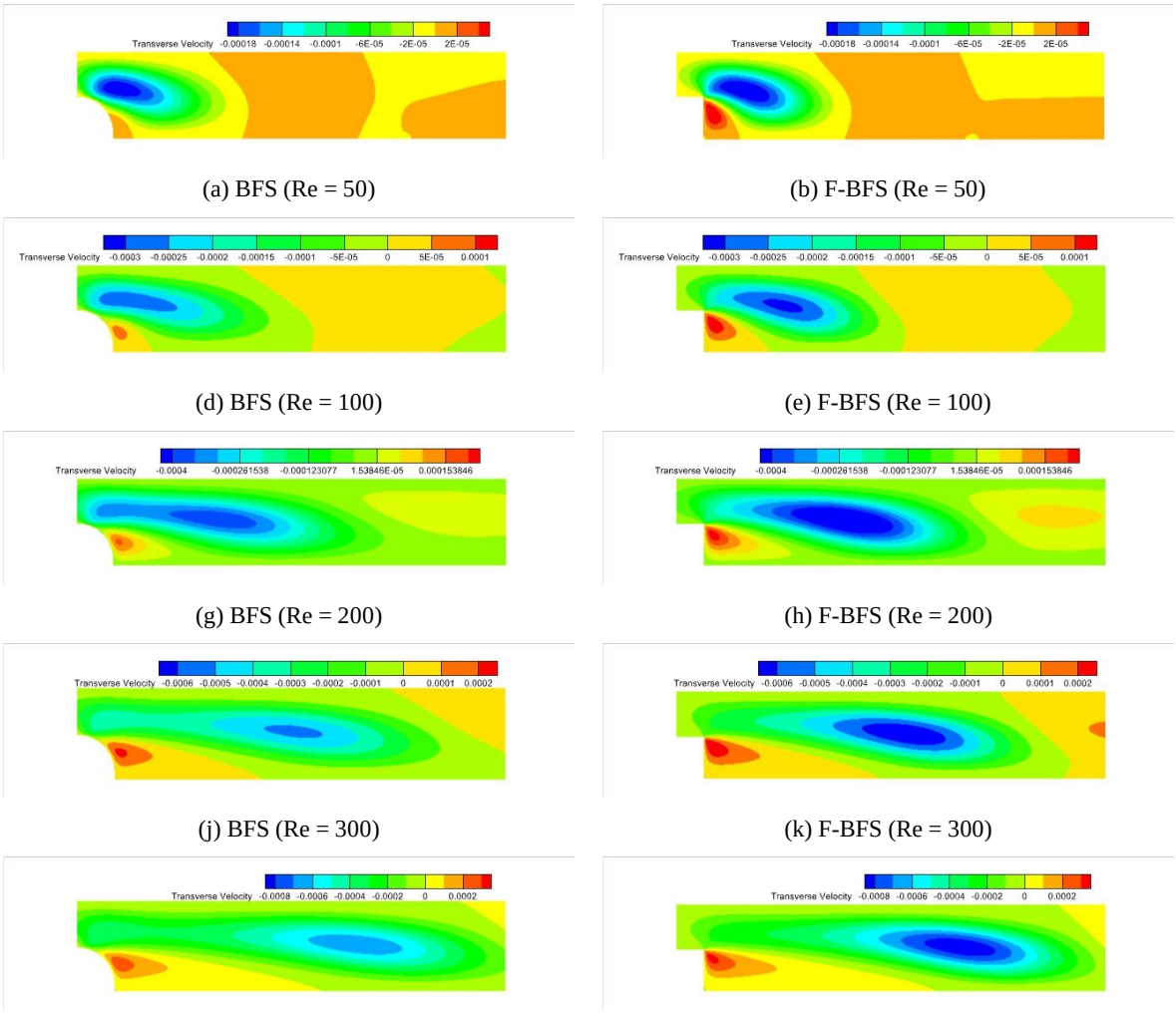

(a) BFS (Re = 50) (b) F-BFS (Re = 50)

(d) BFS (Re = 100) (e) F-BFS (Re = 100)

(g) BFS (Re = 200) (h) F-BFS (Re = 200)

(j) BFS (Re = 300) (k) F-BFS (Re = 300)

(l) BFS (Re = 400) (m) F-BFS (Re = 400)

Figure 6. Transverse velocity contour of backward facing step flow

The flow separation causes a significant change in velocity gradient and affects the flow pattern that passes through the BFS. In Figure 7, a streamline contour is shown to provide further understanding regarding the characteristics of the flow pattern through the BFS. In the streamline contour, it can be seen that the flow separation that occurs forms a vortex that continues to grow as the Reynolds number increases. The formed vortex has wholly covered the step height to be called a recirculation area. The size of the recirculation area can be measured by determining the location of the reattachment point on the downstream side, as seen in Figure 8. The reattachment point can be defined as the point where the fluid returns to touch the surface wall of the channel. In Figure 8, it can be seen that the increase in the size of the recirculation area forms an almost linear increase curve for the two samples. In general, the non-linear conditions in the increase in the recirculation area are caused by the viscosity properties of the boundary conditions. The size of the recirculation area that occurs in BFS is more significant than in F-BFS. In addition, at Re=400, secondary recirculation begins to be seen in the flow that passes through BFS. This condition is due to an abrupt change in the geometric standard form of the BFS. By using the fillet shape as a step, the size of the recirculation area can be appropriately minimized.

In general, the recirculation area that occurs tends to form a vortex pattern that rotates unstable it will disrupt the efficiency level of the internal flow. The efficiency of the internal flow through the BFS can generally be seen from the resulting pressure losses. In Figure 9, the pressure coefficient distribution is displayed along the channel wall on the upstream and downstream sides for each Reynolds number. It can be seen that the maximum pressure is reached at the inlet of the channel. For both samples, the distribution of the resulting pressure coefficient on the upstream side tends to be identical.

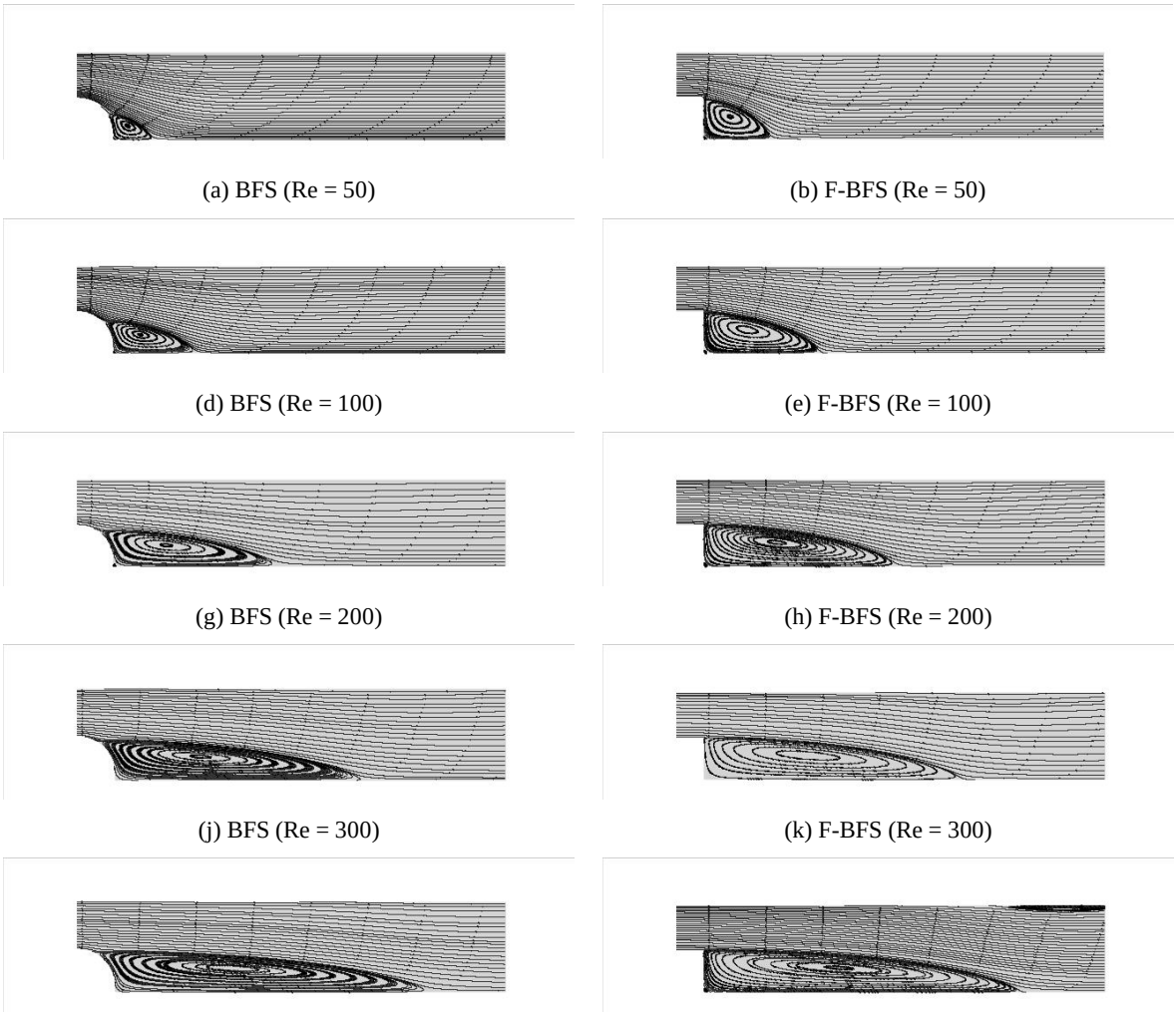

(a) BFS (Re = 50) (b) F-BFS (Re = 50)

(d) BFS (Re = 100) (e) F-BFS (Re = 100)

(g) BFS (Re = 200) (h) F-BFS (Re = 200)

(j) BFS (Re = 300) (k) F-BFS (Re = 300)

(l) BFS (Re = 400) (m) F-BFS (Re = 400)

Figure 7. Streamline velocity contour of backward facing step flow

On the upstream side, there is a linear decrease in the pressure coefficient for the two samples with different gradients for each Reynold number used. Differences in the conditions of the two samples begin to appear when the fluid has passed the step on the downstream side. There is a significant increase in the pressure coefficient in the recirculation area. The increase in pressure coefficient in this area follows Bernoulli's principle, which is associated with a decrease in average speed due to sudden expansion changes [17]–[20]. In addition, the increase in pressure coefficient is also caused by the recirculation area, which has a velocity in the opposite direction to the flow direction, affecting the motion between fluid particles. In Figure 9, the gradient of increasing pressure coefficient can be minimized by changing geometric shapes such as F-BFS. Thus, F-BFS exhibits more efficient fluid flow characteristics than BFS.

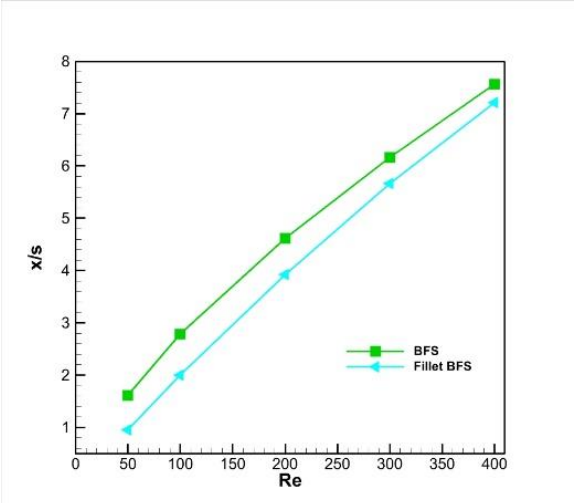

Figure 8. The location of the reattachment points behind the step normalized by the step height S

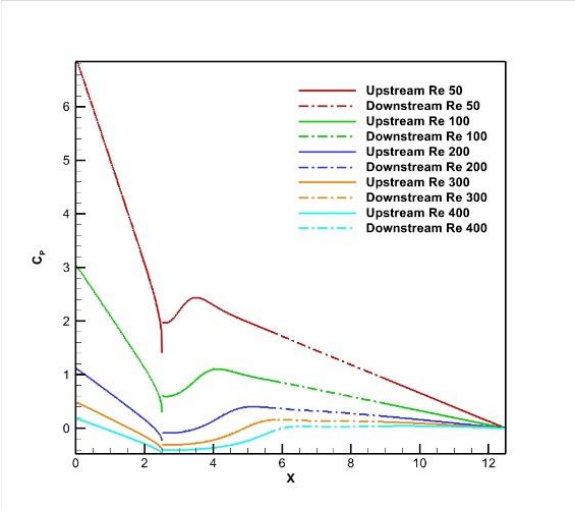

(a) BFS

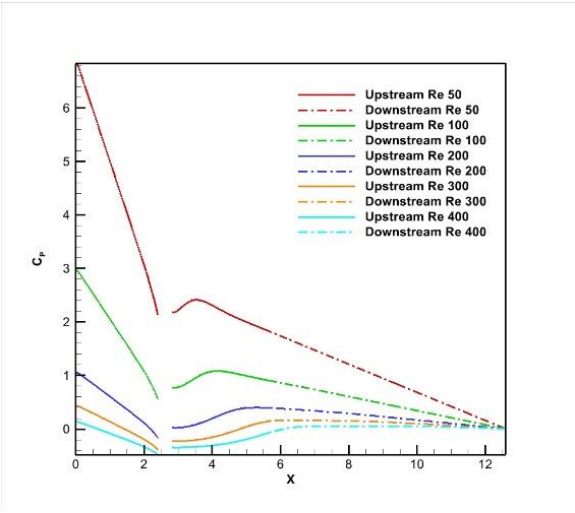

(b) F-BFS

Figure 9. Pressure coefficient distribution of backward facing step

4. Conclusion

This research investigates the effect of the step shape on the internal flow characteristics of the fluid flowing through the backward-facing step. The fillet backward-facing step (F-BFS) shape was chosen with a smoother surface angle. Fluid flow characteristics are tested at intervals of Reynolds number (50<Re<400) through two-dimensional numerical computation. Based on the computational results, flow separation is vital in determining the characteristics produced by the BFS flow. For every increase in the Reynolds number, there is an almost linear increase in flow separation. F-BFS has shape properties that can minimize flow separation that occurs. These properties are proven based on the reattachment points generated by the two samples. In a streamlined contour, flow separation forms a recirculation area that contains unstable rotating vortexes. Therefore, the recirculation area can affect the efficiency of the internal flow in the channel. The efficiency of the internal flow that passes through the BFS is reviewed through the distribution of the resulting pressure coefficient. Based on the distribution of the resulting pressure coefficient, it can be proven that there is a significant gradient increase in the coefficient when in the recirculation area. The pressure coefficient increase gradient is proven to be minimized by F-BFS. Thus, using a step shape with a smoother surface angle can increase the efficiency of the internal flow through the BFS.

References

[1] L. Chen, K. Asai, T. Nonomura, G. Xi, and T. Liu, "A review of Backward-Facing Step (BFS) flow mechanisms, heat transfer and control," Thermal Science and Engineering Progress, vol. 6, pp. 194–216, 2018, doi: https://doi.org/10.1016/j.tsep.2018.04.004.

[2] D. Yang, B. Sun, T. Xu, B. Liu, and H. Li, "Experimental and numerical study on the flow and heat transfer characteristic of nanofluid in the recirculation zone of backward-facing step microchannels," Appl Therm Eng, vol. 199, p. 117527, 2021, doi: https://doi.org/10.1016/j.applthermaleng.2021.117527.

[3] G. Guo, H. Liu, and B. Zhang, "Numerical study of active flow control over a hypersonic backward-facing step using supersonic jet in near space," Acta Astronaut, vol. 132, pp. 256–267, 2017, doi: https://doi.org/10.1016/j.actaastro.2016.12.035.

[4] R. Huang, X. Luo, B. Ji, and J. Qingfeng, "Turbulent Flows Over a Backward Facing Step Simulated Using a Modified Partially Averaged Navier–Stokes Model," J Fluids Eng, vol. 139, May 2016, doi: 10.1115/1.4035114.

[5] S. Scharnowski, I. Bolgar, and C. Kähler, "Characterization of Turbulent Structures in a Transonic Backward-Facing Step Flow," Flow Turbul Combust, vol. 98, May 2017, doi: 10.1007/s10494-016-9792-8.

[6] A. Sivan, D. Saravanan, and Y. S. Rammohan, "A numerical study to reduce the drag effects in hypersonic flow over the backward facing step," Mater Today Proc, vol. 52, pp. 963–970, 2022, doi: https://doi.org/10.1016/j.matpr.2021.10.429.

[7] J. Morita, H. Mamori, and T. Miyazaki, "Direct numerical simulation of the backward-facing step turbulent flow controlled by traveling wave-like body force," Int J Heat Fluid Flow, vol. 95, p. 108964, 2022, doi: https://doi.org/10.1016/j.ijheatfluidflow.2022.108964.

[8] T. McQueen, D. Burton, J. Sheridan, and M. C. Thompson, "Active control of flow over a backward-facing step at high Reynolds numbers," Int J Heat Fluid Flow, vol. 93, p. 108891, 2022, doi: https://doi.org/10.1016/j.ijheatfluidflow.2021.108891.

[9] G. Biswas, M. Breuer, and F. Durst, "Backward-Facing Step Flows for Various Expansion Ratios at Low and Moderate Reynolds Numbers," J Fluids Eng, vol. 126, no. 3, pp. 362–374, Jul. 2004, doi: 10.1115/1.1760532.

[10] S. Inam and M. Lappa, "Hybrid forced-buoyancy convection in a channel with a backward facing step," Int J Heat Mass Transf, vol. 194, p. 122963, 2022, doi: https://doi.org/10.1016/j.ijheatmasstransfer.2022.122963.

[11] G. Guo, H. Liu, and B. Zhang, "Numerical study of active flow control over a hypersonic backward-facing step using supersonic jet in near space," Acta Astronaut, vol. 132, pp. 256–267, May 2017, doi: 10.1016/j.actaastro.2016.12.035.

[12] B. Armaly, F. Durst, J. Pereira, and B. Schönung, "Experimental and Theoretical Investigation of Backward-Facing Step Flow," J Fluid Mech, vol. 127, pp. 473–496, May 1983, doi: 10.1017/S0022112083002839.

[13] A. S. A. N. D. R. N. A. A. N. D. A. K. A. Aftab S. M. A. AND Mohd Rafie, "Turbulence Model Selection for Low Reynolds Number Flows," PLoS One, vol. 11, no. 4, pp. 1–

15, May 2016, doi: 10.1371/journal.pone.0153755.
[14] J. Julian, W. Iskandar, F. Wahyuni, A. Armansyah, and F. Ferdyanto, "Effect of Single Slat and Double Slat on Aerodynamic Performance of NACA 4415," International Journal of Marine Engineering Innovation and Research, vol. 7, no. 2, 2022.
[15] J. Julian, W. Iskandar, and F. Wahyuni, "COMPUTATIONAL FLUID DYNAMICS ANALYSIS BASED ON THE FLUID FLOW SEPARATION POINT ON THE UPPER SIDE OF THE NACA 0015 AIRFOIL WITH THE COEFFICIENT OF FRICTION," Jurnal Media Mesin, vol. 23, no. 2.
[16] P. J. Roache, "Perspective: a method for uniform reporting of grid refinement studies," 1994.
[17] J. Julian, W. Iskandar, and F. Wahyuni, "Aerodynamics Improvement of NACA 0015 by Using Co-Flow Jet," International Journal of Marine Engineering Innovation and Research, vol. 7, pp. 1479–2548, Mar. 2022, doi: 10.12962/j25481479.v7i4.14898.
[18] J. Julian, W. Iskandar, F. Wahyuni, and N. T. Bunga, "Aerodynamic Performance Improvement on NACA 4415 Airfoil by Using Cavity," Jurnal Asiimetrik: Jurnal Ilmiah Rekayasa Dan Inovasi, vol. 5, no. 1, Jan. 2023, doi: 10.35814/asiimetrik.v5i1.4259.
[19] J. Julian, W. Iskandar, F. Wahyuni, and N. T. Bunga, "Characterization of the Co-Flow Jet Effect as One of the Flow Control Devices," Jurnal Asiimetrik: Jurnal Ilmiah Rekayasa & Inovasi, pp. 185–192, 2022.
[20] W. Iskandar, J. Julian, F. Wahyuni, F. Ferdyanto, H. Prabu, and F. Yulia, "Study of Airfoil Characteristics on NACA 4415 with Reynolds Number Variations," International Review on Modelling and Simulations (IREMOS), vol. 15, p. 162, Feb. 2022, doi: 10.15866/iremos.v15i3.21684.